Journal Name

Molecular electrometer and binding of cations to phospholipid bilayers[†]

Andrea Catte,[a‡] Mykhailo Girych,[b] Matti Javanainen,[c,d] Claire Loison,[e] Josef Melcr,[f] Markus S. Miettinen,[g,h] Luca Monticelli,[i] Jukka Määttä,[j] Vasily S. Oganesyan,[a] O. H. Samuli Ollila,[*b] Joona Tynkkynen,[c] and Sergey Vilov,[e]

Despite the vast amount of experimental and theoretical studies on the binding affinity of cations into phospholipid bilayers, especially the biologically relevant Na^+ and Ca^{2+} ions, there is no consensus in the literature. In this paper, we show that the ion binding affinity can be directly compared between simulations and experiments by using the choline headgroup order parameters according to the 'molecular electrometer' concept [Seelig *et al., Biochemistry*, 1987, **26**, 7535]. Our findings strongly support the view that Na^+ and other monovalent ions (except Li^+) do not specifically bind to phosphatidylcholine lipid bilayers with sub-molar concentrations, in contrast to Ca^{2+} and other multivalent ions. Especially the Na^+ binding affinity is overestimated by several molecular dynamics simulation models, leading to an artificially positively charged lipid bilayer and exaggerated structural effects in the headgroups. Qualitatively correct headgroup order parameter response is observed with Ca^{2+} binding in all the tested models, however, none of them has a sufficient quantitative accuracy to interpret the Ca^{2+}:lipid stoichiometry or the induced atomistic resolution structural changes. This work has been done as a fully open collaboration, using `nmrlipids.blogspot.fi` as a main communication platform; all the scientific contributions were made publicly on this blog.

1 Introduction

Due to its high physiological importance — nerve cell signalling being the prime example — interaction of cations with phospholipid membranes has been widely studied via theory, simulations, and experiments. The relative ion binding affinities are gener-

ally agreed to follow the Hofmeister series[1–9], however, consensus on the quantitative affinities is currently lacking. Until 1990, the consensus (documented in two extensive reviews[2,3]) was that while multivalent cations interact significantly with phospholipid bilayers, for monovalent cations (with the exception of Li^+) the interactions are weak. This conclusion has since been strengthened by further studies showing that bilayer properties remain unaltered upon the addition of sub-molar concentrations of monovalent salt[4,10,11]. Since 2000, however, another view has emerged, suggesting much stronger interactions between phospholipids and monovalent cations, and strong Na^+ binding in particular[6–9,12–18].

The pre-2000 view has the experimental support that (in contrast to the significant effects caused by any multivalent cations) sub-molar concentrations of NaCl have a negligible effect on phospholipid infrared spectra[4], area per molecule[10], dipole potential[19], lateral diffusion[11], and choline head group order parameters[20]; in addition, the water sorption isotherm of a NaCl–phospholipid system is highly similar to that of a pure NaCl solution — indicating that the ion–lipid interaction is very weak[4].

The post-2000 'strong binding' view rests on experimental and above all simulation findings. At sub-molar NaCl concentrations, the rotational and translational dynamics of membrane-

[a] School of Chemistry, University of East Anglia, Norwich, NR4 7TJ, United Kingdom

[b] Department of Neuroscience and Biomedical Engineering, Aalto University, Espoo, Finland

[c] Tampere University of Technology, Tampere, Finland

[d] University of Helsinki, Helsinki, Finland

[e] Univ Lyon, Université Claude Bernard Lyon 1, CNRS, Institut Lumiére Matiére, F-69622, LYON, France

[f] Institute of Organic Chemistry and Biochemistry, Czech Academy of Sciences, Flemingovo nám. 2, 16610 Prague 6, Czech Republic, Charles University in Prague, Faculty of Mathematics and Physics, Ke Karlovu 3, 121 16 Prague 2, Czech Republic

[g] Fachbereich Physik, Freie Universität Berlin, Berlin, Germany

[h] Max Planck Institute of Colloids and Interfaces, Department of Theory and Bio-Systems, Potsdam, Germany

[i] Institut de Biologie et Chimie des Protéines (IBCP), CNRS UMR 5086, Lyon, France

[j] Aalto University, Espoo, Finland

[*]**Author to whom correspondence may be addressed.** E-mail: samuli.ollila@aalto.fi.

† Electronic Supplementary Information (ESI) available: 5 figures, detailed technical discussion and simulation details. See DOI: 10.1039/b000000x/

‡ The authors are listed in alphabetical order.

embedded fluorescent probes decrease[7,9,12], and atomic force microscopy (AFM) experiments show changes in bilayer hardness[14–18]; in atomistic molecular dynamics (MD) simulations, phospholipid bilayers consistently bind Na$^+$, although the binding strength depends on the model used[12,13,21–26].

Some observables have been interpreted in favour of both views. For example, as the effect of monovalent ions (except Li$^+$) on the phase transition temperature is tiny (compared to the effect of multivalent ions), it was initially interpreted as an indication that only multivalent ions and Li$^+$ specifically bind to phospholipid bilayers[2]; however, such a small effect in calorimetric measurements was later interpreted to indicate that also Na$^+$ binds[8,12]. Similarly, the lack of significant positive electrophoretic mobility of phosphatidylcholine (PC) vesicles in the presence of NaCl (again in contrast to multivalent ions and Li$^+$) suggested weak binding of Na$^+$[1,8,14,15,27]; however, these data have also been explained by a countering effect of the Cl$^-$ ions[22,28]. To reduce the area per lipid in scattering experiments, molar concentrations of NaCl are required[10], which indicates weak ion–lipid interaction; in MD simulations, however, already orders of magnitude lower concentrations result in Na$^+$ binding and clear reduction of area per lipid[12,23]. Finally, in noninvasive NMR experiments, lipid lateral diffusion is unaltered by NaCl[11]; however, it is reduced in simulations upon Na$^+$ binding, which supports interpreting the reduced lateral diffusion of fluorescent probes[7,9,12] as favouring the post-2000 view.

In this paper we set out to solve the apparent contradictions between the pre-2000 and post-2000 views. To this end we employ the 'molecular electrometer' concept, according to which the changes in the order parameters of the α and β carbons in the phospholipid head group (see Fig. 1) can be used to measure the ion affinity to PC lipid bilayer[20,29?–31]. As order parameters can be accurately measured in experiments and directly compared to simulations[32], employing the molecular electrometer as a function of cation concentration allows the comparison of binding affinity between simulations and experiments. In addition to demonstrating the usefulness of this general concept, we show that the response of order parameters to penetrating cations is qualitatively correct in MD simulations, but that in several models the affinity of Na$^+$ for PC bilayers is grossly overestimated. Moreover, we show that the accuracy of lipid–Ca^{2+} interactions in current models is not enough for atomistic resolution interpretation of NMR experiments.

This work has been done as an Open Collaboration at `nmrlipids.blogspot.fi`; all the related files[129] and almost all the simulation data (`https://zenodo.org/collection/user-nmrlipids`) are openly available.

2   Results and Discussion

2.1   Background: Molecular electrometer in experiments

The molecular electrometer concept is based on the experimental observation that binding of any charged objects (e.g. ions, peptides, anesthetics, amphihiles) on a PC bilayer interface induces systematic changes in the choline β and α segment order parameters[20,29–31,33?–38]. Thus, these changes can be used to
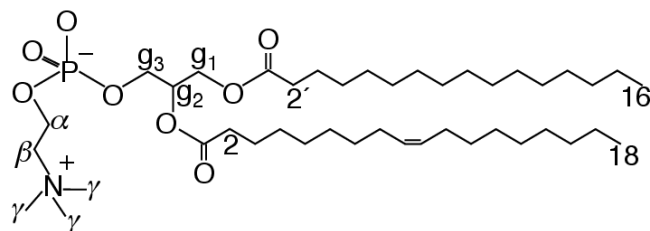

Fig. 1 Chemical structure of 1-palmitoyl-2-oleoylphosphatidylcholine (POPC), and the definition of γ, β, α, g_1, g_2 and g_3 segments.

determine binding affinities of the charged objects. The molecular electrometer was originally devised for cations[20,29?], but further experimental quantification with various positively and negatively charged molecules showed that the choline order parameters S_{CH}^{α} and S_{CH}^{β} in general vary linearly with small amount of bound charge per lipid[29–31,33–38]. The empirically observed linear relation can be written as[39]

$$S_{CH}^i(X^\pm) = S_{CH}^i(0) + \frac{4m_i}{3\chi}X^\pm, \qquad (1)$$

where $S_{CH}^i(0)$ is the order parameter in the absence of bound charges, m_i is an empirical constant depending on the valency and position of bound charge, $X^\pm$ is the amount of the bound charge per lipid, i refers to either α or β, and the value of quadrupole coupling constant is $\chi \approx 167$ kHz. The change in order parameters with respect to a bilayer without bound charges then becomes

$$\Delta S_{CH}^i = S_{CH}^i(X^\pm) - S_{CH}^i(0) = \frac{4m_i}{3\chi}X^\pm. \qquad (2)$$

For Ca^{2+} binding to POPC bilayer (in the presence of 100 mM NaCl), combination of atomic absorption spectra and ^{2}H NMR experiments gave $m_\alpha = -20.5$ and $m_\beta = -10.0$[29].

The absolute values of order parameters increase for β and decrease for α segment with bound positive charge and *vice versa* for negative charge[20,29–31,33,38?]. However, as the β carbon order parameter is negative while α carbon order parameter is positive[40–42], we can conclude that both ΔS_{CH}^{β} and ΔS_{CH}^{α} decrease with bound positive charge and increase with bound negative charge. Consequently, values of m_i are negative for bound positive charges and *vice versa*. This can be rationalised by electrostatically induced changes in choline P–N dipole tilt[30,31,44], which is also seen in simulations[23,24,45,46]. This is in line with order parameter decrease related to the P–N vector tilting more parallel to membrane plane seen with decreasing hydration levels[43].

The quantification of ΔS_{CH}^{β} and ΔS_{CH}^{α} with different cations have revealed that $\Delta S_{CH}^{\beta}/\Delta S_{CH}^{\alpha} \approx 0.5$ for a wide range of different cations (aqueous cations, cationic peptides, cationic anes-
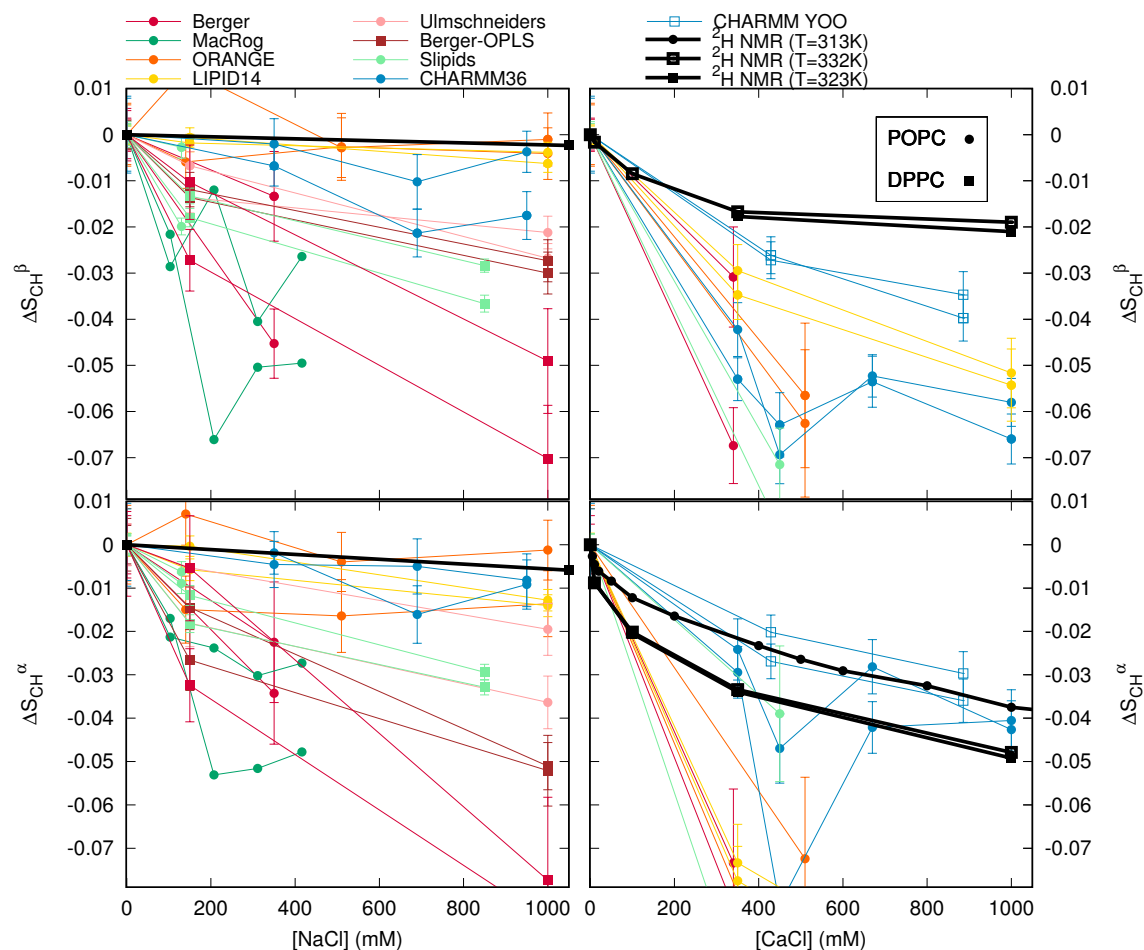
Fig. 2 The order parameter changes for β and α segments as a function of NaCl (left column) and CaCl$_2$ (right column) concentration, from simulations and experiments[20] (POPC with CaCl$_2$ from[29]). The signs of the experimental order parameters, taken from experiments without ions[40–42], can be assumed to be unchanged with concentrations represented here[29,32]. It should be noted that none of the models used here reproduces the order parameters within experimental error for pure PC bilayer without ions, indicating structural inaccuracies with varying severity in all models[43]. Note that the relatively large decrease in CHARMM36 with 450 mM CaCl$_2$ arise from more equilibrated binding affinity due to long simulation times, see ESI†.

thetics)[36,38]. More specifically, the relation $\Delta S_{CH}^{\beta} = 0.43 \Delta S_{CH}^{\alpha}$ was found for a DPPC bilayer with various CaCl$_2$ concentrations[20].

2.2 Molecular electrometer concept in MD simulations

The headgroup order parameter changes as a function of ion concentration in solution from H^2 NMR experiments are shown in Fig. 2 for DPPC and POPC bilayers[20,29]. Only minor changes in order parameters are seen as a function of NaCl in solution, while the effect of CaCl$_2$ is an order of magnitude larger. Thus, according to the molecular electrometer concept, monovalent Na$^+$ ions have negligible affinity for PC lipid bilayers at concentrations up to 1 M, while binding of Ca^{2+} ions at the same concentration is significant[20,29].

Figure 2 also reports order parameter changes calculated from MD simulations of DPPC and POPC lipid bilayers as a function of NaCl or CaCl$_2$ initial concentrations in solution (for details of the simulated systems see Table 1 and ESI†). Note that none of these MD models reproduced within experimental uncertainty the order parameters for a pure PC bilayer without ions (Figure 2 in Ref. 43), indicating structural inaccuracies of varying severity in

all models[43]. However, the experimentally observed headgroup order parameter increase with dehydration was qualitatively reproduced by all the models[43], and similarly here the presence of cations leads to the decrease of S_{CH}^{β} and S_{CH}^{α} (Fig. 2), in qualitative agreement with experiments. The changes are, however, overestimated by most models. According to the electrometer concept this indicates overbinding of cations in most MD simulation models.

While electrometer concept is well established in experiments (see previous section), it is not *a priori* clear that it works in simulations. The overestimated order parameter decrease could, in principle, arise also from the oversensitivity of choline headgroups on cation binding, instead of overbinding. Here we analyse the relation between cation binding and choline order parameter decrease in simulations in order to evaluate the usability of the electrometer concept in MD simulations.

According to the molecular electrometer concept, order parameter changes are linearly proportional to the amount of bound cations in bilayer (Eq. (2)). Figure 3 shows the changes in order parameter as a function of bound charge in MD simula-
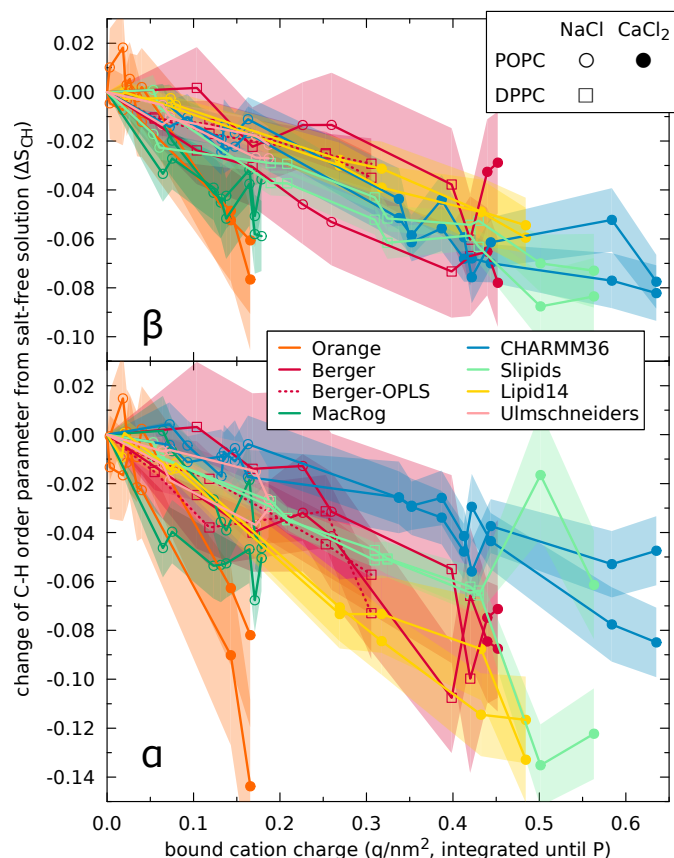
Fig. 3 Change of order parameters (from salt-free solution) of the β and α segments, ΔS_{CH}^{β} and ΔS_{CH}^{α}, as a function of bound cation charge. Eight MD simulation models compared; the two lines per model denote to the two hydrogens per carbon. The order parameters as well as the bound charge calculated separately for each leaflet; cations residing between the bilayer centre and the density maximum of Phosphorus considered bound; error bars (shaded) show standard error of mean over lipids.

tions (see ESI[†] for the definition of bound ions); in keeping with the molecular electrometer, roughly linear correlation between bound charge and order parameter change is found in all models. Note that quantitative comparison of the proportionality constants (i.e. slopes in Fig. 3) between different models and experimental slopes ($m_\alpha = -20.5$ and $m_\beta = -10.0$ for Ca^{2+} binding in DPPC bilayer in the presence of 100mM NaCl in Eq. 1[29]) is not straightforward since the simulation slopes depend on the definition used for bound ions (see ESI[†]).

The comparison of order parameter changes in response to bound charge is more straightforward for systems with charged amphiphiles fully associated in bilayer, as the amount of bound charge is then explicitly known in both simulations and experiments. Such comparison between previously published simulation data[47] and experiments[31,48] could not rule out overestimation of order parameter response to bound cations (i.e., slopes m_β and m_α) in a Berger-based model (ESI[†]). This might, in principle, explain the overestimated order parameter response of Berger model to $CaCl_2$, but not to NaCl (see discussion in ESI[†]). Since simulation data with charged amphiphiles from other models is not available, the extended comparison with different models is

left for further studies.

Figure 3 shows that the decrease on order parameter clearly correlates with the amount of bound cations also in simulations. This is also evident from Fig. 4, which shows the Na^+ density profiles of the MD models ordered according to the order parameter change (reported in Fig. 2) from the smallest (top) to the largest (bottom). The Na^+ density peaks are larger for models with larger changes in order parameters, in line with the observed correlation between cation binding and order parameter decrease in Fig. 3.

Figure 5 compares the relation between ΔS_{CH}^{β} and ΔS_{CH}^{α} in experiments[20] and different simulation models. Only Lipid14 gives $\Delta S_{CH}^{\beta}/\Delta S_{CH}^{\alpha}$ ratio in agreement with the experimental ratio. In all the other models the α order parameter decrease with bound cations is underestimated with respect to β order parameter decrease.

In conclusion, the clear correlation between bound cations and order parameter decrease is observed in all the tested simulation models. Consequently, the electrometer concept can be used to compare the cation binding affinity between experiments and simulations. However, we find that the quantitative response of α and β segment order parameters to bound cations in simulations do not generally agree with the experiments. The $\Delta S_{CH}^{\beta}/\Delta S_{CH}^{\alpha}$ ratio agrees with experiments only in Lipid14 model (Fig. 5). Thus, the observed overestimation of the order parameter changes with cation concentrations may, in principle, arise from overbinding of ions or from too sensitive lipid headgroup response on bound cation (see also discussion in ESI[†]). A careful analysis with current lipid models is performed in the next section.

2.3 Cation binding in different simulation models

The order parameter changes (Fig. 2) and density distributions (Fig. 4) demonstrate significantly different Na^+ binding affinities in different simulation models. The best agreement with experiments (lowest ΔS_{CH}^{α} and ΔS_{CH}^{β}) is observed for those models (Orange, CHARMM36, and Lipid14; see Fig. 2) that also predict the lowest Na^+ densities in the membrane proximity (Fig. 4). In all the other tested models, the choline order parameter responses to NaCl are clearly overestimated (Fig. 2), and the strength of the overestimation is clearly linked to the strength of the Na^+ binding affinity (compare Figs. 2 and 4); this leads us to conclude that sodium binding affinity is overestimated in all these models.

In the best three models, the order parameter changes with NaCl are small (< 0.02), so with the achieved statistical accuracy we cannot conclude which of the three has the most realistic Na^+ binding affinity, especially at physiological NaCl concentrations (~ 150mM) relevant for most applications. The overestimated binding in the other models raise questions on the quality of the predictions from these models when NaCl is present. Especially interactions between charged molecules and lipid bilayer might be significantly affected by the strong Na^+ binding, as it makes the bilayer effectively positively charged.

Significant Ca^{2+} binding affinity to a phosphatidylcholine bilayer at sub-molar concentrations is agreed in the literature[2,3,20,29], however, several details are yet under discussion.

Table 1 List of MD simulations. The salt concentrations calculated as [salt]=$N_c \times$[water]/N_w, where [water] = 55.5 M; these correspond the concentrations reported in the experiments by Akutsu et al.[20]. The lipid force fields named as in our previous work[43].

Force field (lipid, ion)	lipid	salt	[salt] (mM)	$^a N_l$	$^b N_w$	$^c N_c$	$^d T$ (K)	$^e t_{sim}$ (ns)	$^f t_{anal}$ (ns)	^{g}Files
Berger-POPC-07[49]	POPC	no	0	128	7290	0	298	270	50	50
Berger-POPC-07[49], ffgmx[51]	"	NaCl	340	"	7202	44	"	110	"	52
Berger-POPC-07[49], ffgmx[51]	"	CaCl$_2$	340	"	7157	44	"	108	58	53
Berger-DPPC-97[54]	DPPC	no	0	72	2880	0	323	60	50	55
Berger-DPPC-97[54], ffgmx[51]	"	NaCl	150	"	"	8	"	120	60	56
Berger-DPPC-97[54], ffgmx[51]	"	"	1000	"	2778	51	"	"	"	57
BergerOPLS-DPPC-06[58]	DPPC	no	0	72	2880	0	323	120	60	59
BergerOPLS-DPPC-06[58], OPLS[60]	"	NaCl	150	"	"	8	"	"	"	61
BergerOPLS-DPPC-06[58], OPLS[60]	"	"	1000	"	2778	51	"	"	"	62
CHARMM36[63]	POPC	no	0	128	5210	0	303	200	150	?
CHARMM36[63]	"	"	0	72	2242	0	"	30	20	64
CHARMM36[63], CHARMM36[65]	"	NaCl	350	"	2085	13	"	80	60	66
CHARMM36[63], CHARMM36[65]	"	"	690	"	"	26	"	73	"	67
CHARMM36[63], CHARMM36[65]	"	"	950	"	2168	37	"	80	"	68
CHARMM36[63], CHARMM36	"	CaCl$_2$	350	128	6400	35	"	200	100	69
CHARMM36[63], CHARMM36	"	"	450	200	9000	73	310	2000	"	70
CHARMM36[63], CHARMM36	"	"	670	128	6400	67	303	200	120	71
CHARMM36[63], CHARMM36	"	"	1000	"	"	100	"	"	100	72
CHARMM36[63]	DPPC	no	0	128	8000	0	323	170	150	–
CHARMM36[63], Yoo[73]	"	CaCl$_2$	430	"	7760	60	"	200	170	–
CHARMM36[63], Yoo[73]	"	"	890	"	7520	120	"	"	"	–
MacRog[74]	POPC	no	0	128	6400	0	310	400	200	?
MacRog[74]	"	"	0	288	14400	0	"	90	40	75
MacRog[74], OPLS[60]	"	NaCl	100	"	14554	27	"	"	50	76
MacRog[74], OPLS[60]	"	"	210	"	14500	54	"	"	"	"
MacRog[74], OPLS[60]	"	"	310	"	14446	81	"	"	"	"
MacRog[74], OPLS[60]	"	"	420	"	14392	108	"	"	"	"
Orange	POPC	no	0	72	2880	0	298	60	50	77
Orange, OPLS[60]	"	NaCl	140	"	2866	7	"	120	60	78
Orange, OPLS[60]	"	"	510	"	2802	26	"	"	100	79
Orange, OPLS[60]	"	"	1000	"	2780	50	"	"	80	80
Orange, OPLS	"	CaCl$_2$	510	"	2802	26	"	"	60	81
Slipids[87]	POPC	no	0	128	5120	0	310	200	150	88
Slipids[87], AMBER[89]	"	NaCl	130	200	9000	21	"	105	100	90
Slipids[87], AMBER[60]	"	CaCl$_2$	450	"	"	73	"	2000	"	91
Slipids[82]	DPPC	no	0	128	3840	0	323	150	100	83
Slipids[82], AMBER[84,85]	"	NaCl	150	600	18000	49	"	100	40	–
Slipids[82], AMBER[84,85]	"	"	850	128	3726	57	"	205	200	86
Slipids[82], AMBER[84,85]	"	"	1750	"	3612	114	"	105	100	"
Slipids[82], AMBER[84,85]	"	"	2570	"	3514	163	"	"	"	"
Lipid14[92]	POPC	no	0	128	5120	0	298	205	200	93
Lipid14[92], AMBER[60]	"	NaCl	150	"	"	12	"	"	"	94
Lipid14[92], AMBER[60]	"	"	1000	"	"	77	"	"	"	95
Lipid14[92], AMBER[60]	"	CaCl$_2$	350	"	6400	35	"	200	100	96
Lipid14[92], AMBER[60]	"	"	1000	"	"	100	"	"	"	97
Ulmschneiders[98]	POPC	no	0	128	5120	0	298	2×205	2×200	99
Ulmschneiders[98], OPLS[60]	"	NaCl	150	"	"	12	"	205	200	100
Ulmschneiders[98], OPLS[60]	"	"	1000	"	"	77	"	"	"	101

a The number of lipid molecules
b The number of water molecules
c The number of cations
d Simulation temperature
e The total simulation time
f Time frames used in the analysis
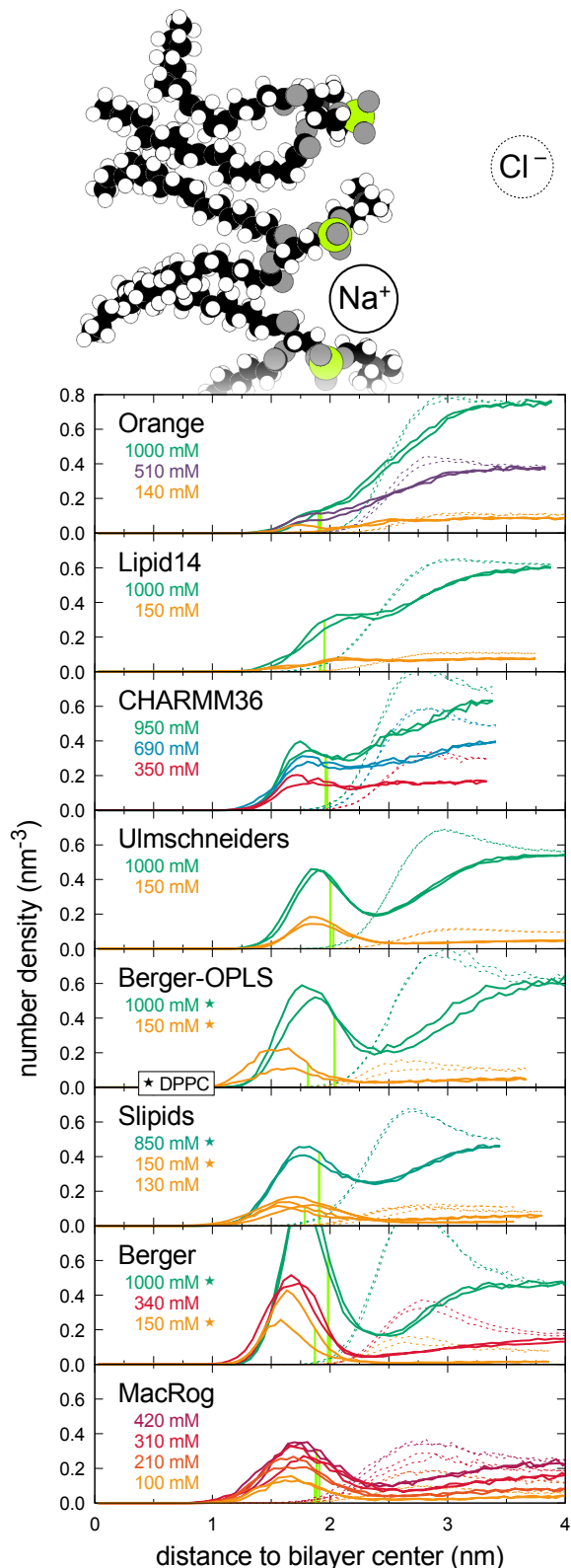g Reference for simulation files

Fig. 4 Na$^+$ (solid line) and Cl$^-$ (dashed) distributions along the lipid bilayer normal from MD simulations at several NaCl concentrations. The eight MD models are ordered according to their strength of order parameter change in response to NaCl (Fig. 2) from the weakest (top panel) to the strongest (bottom). The light green vertical lines indicate the locations of the Phosphorus maxima, used to define bound cations in Fig. 3.
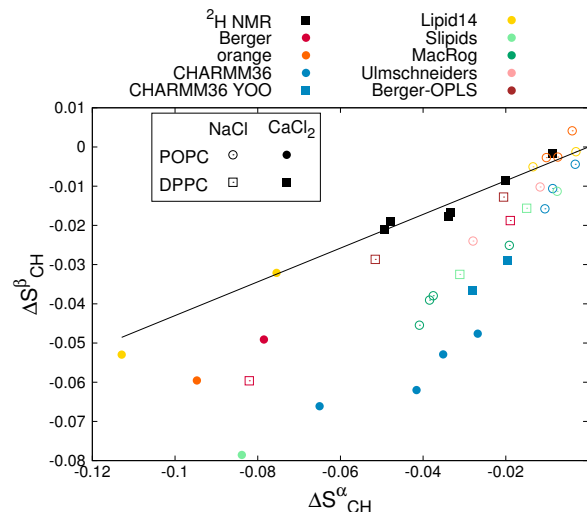

Fig. 5 Relation between ΔS_{CH}^{β} and ΔS_{CH}^{α} from experiments[20] and different simulation models. Solid line is $\Delta S_{CH}^{\beta} = 0.43 \Delta S_{CH}^{\alpha}$ determined for DPPC bilayer from ^{2}H NMR experiment with various CaCl$_2$ concentrations[20].

Simulations suggest that Ca^{2+} bind to lipid carbonyl oxygens with coordination number of 4.2[13], while interpretation of NMR and scattering experiments suggest that one Ca^{2+} interacts mainly with choline groups[102–104] of two phospholipid molecules[29]. A simulation model correctly reproducing the order parameter changes would resolve the discussion by giving atomistic resolution interpretation for the experiments.

As a function of CaCl$_2$ concentration, all but one (CHARMM36 with recent ion model by Yoo et al.[73]), model overestimate the order parameter decrease (Fig. 2). According to the molecular electrometer, this indicates overestimated Ca^{2+} binding. This is the most likely scenario for the models where changes in both order parameters were overestimated, however, in the case of CaCl$_2$ we cannot exclude the possibility that the headgroup response is oversensitive to bound cations (see ESI†). In CHARMM36 with ion model by Yoo et al.[73], ΔS_{CH} is overestimated for β but underestimated for α, in line with Fig. 5 where $\Delta S_{CH}^{\beta}/\Delta S_{CH}^{\alpha}$ ratio in CHARMM36 is larger than in experiments. Since we do not know if ΔS_{CH}^{β} or ΔS_{CH}^{α} is more realistic in CHARMM36, we cannot conclude if Ca^{2+} binding is too strong or weak in this simulation model. This could be resolved by comparing CHARMM36 model to the experimental data with known amount of bound charge (e.g., experiments with amphiphilic cations[31,48]), however, such simulation data are not currently available.

The ion density distributions with CaCl$_2$ in Fig. 6 show significant Ca^{2+} binding in all models, however, some differences occur in details. The Berger model predicts deeper penetration depth (density maxima close to ± 1.8 nm) compared to other models (density maxima close to ± 2 nm). The latter value is probably more realistic since ^{1}H NMR and neutron scattering data indicate that Ca^{2+} interacts mainly with the choline group[2,102–104]. In CHARMM36, almost all Ca^{2+} ions present in simulation bind in bilayer indicating strongest binding affinity among the tested models. The difference is not as clear in Fig. 2 because α car-

bon order parameters are the least sensitive to bound charge in CHARMM36 (Fig. 3).
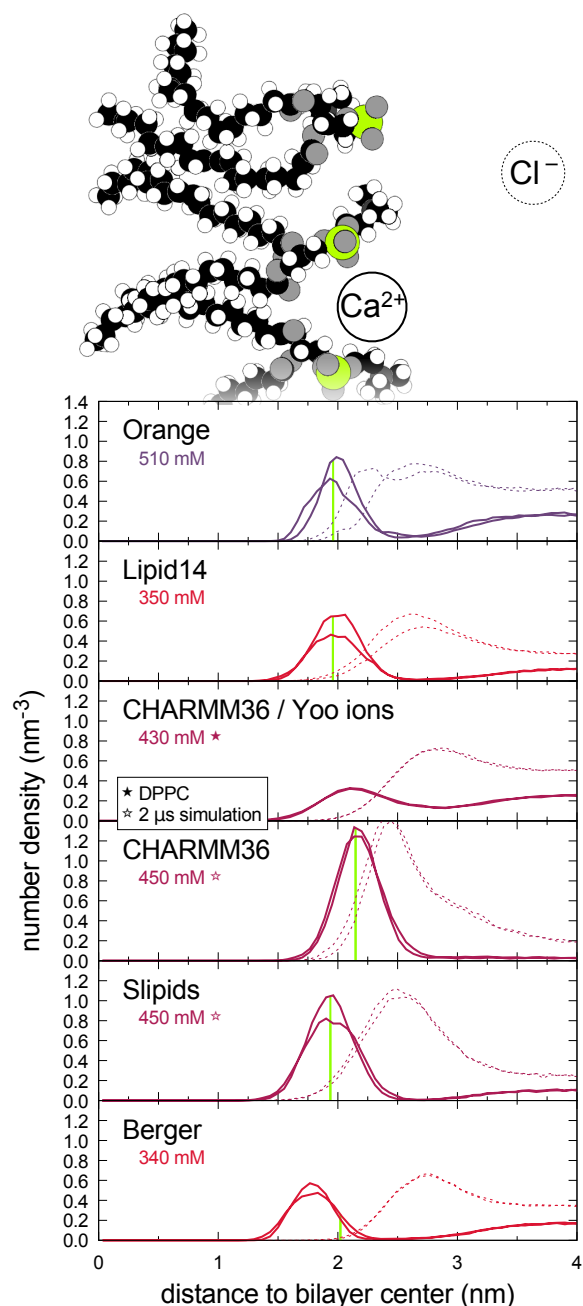

Fig. 6 Ca^{2+} (solid line) and Cl^- (dashed) distributions along the lipid bilayer normal from MD simulations. For clarity, only one $CaCl_2$ concentration per MD model is shown; see ESI† for a plot including all the available concentrations. The light green vertical lines indicate the locations of the Phosphorus maxima, used to define bound cations in Fig. 3.

The origin of inaccuracies in lipid–ion interactions and binding affinities in different models is far from clear. Potential candidates could be, for example, discrepancies in the ion models [105–107], incomplete treatment of electronic polarizability [108], or inaccuracies in the lipid headgroup description [43]. Cordomi et al. [24] showed that the Na^+ binding affinity decreases when ion radius increases in the model, however, also the models with the largest

radius show significant binding in DPPC bilayer simulated with OPLS-AA force field [109]. In our results, the Slipids model gives essentially similar binding affinity with ion parameters from Refs. 89 and 84,85. Further, the compensation of missing electronic polarizability by scaling ion charge [108,110] reduced Na^+ binding in Berger, BergerOPLS and Slipids models, but not enough to be in agreement with experiments (ESI†). The charge-scaled Ca^{2+} model [111] slightly reduced binding in CHARMM36, but did not have significant influence on binding in Slipids (ESI†). Significant reduction of Ca^{2+} binding was observed with ion model by Yoo et al [73], however, the CHARMM36 lipid model must be further analysed to fully interpret the results.

On the other hand, also the lipid models may have significant influence on ion binding behaviour. For example, the same ion model and non-bonded parameters are used in the Orange and BergerOPLS [58] simulations, but while Na^+ ion binding affinity appears realistic in the Orange model, it is significantly overestimated in the BergerOPLS (Fig. 4). However, realistic Na^+ binding does not directly relate to realistic Ca^{2+} binding (see Orange, Lipid14 and CHARMM36 in Fig. 2) or realistic choline order parameter response to bound charge (see Orange and CHARMM36 in Fig. 5). It should be also noted that the low binding affinity of Na^+ in CHARMM36 model is due to the additional repulsion added between sodium ions and lipid oxygens (NBFIX) [65] (ESI†). Altogether, our results indicate that probably both, lipid and ion force field parameters, need improvement to correctly predict the cation binding affinity, and the associated structural changes.

3 Conclusions

As suggested by the molecular electrometer concept [20,29?–31], the decrease in order parameters of α and β carbons in the PC head group of lipids bilayers is related to cation binding in all tested simulation models (Fig. 3), despite of known inaccuracies in the actual atomistic resolution structures [43]. Hence the molecular electrometer concept allows a direct comparison of Na^+ binding affinity between simulations and noninvasive NMR experiments. The comparison reveals that most models overestimate Na^+ binding; only Orange, Lipid14, and CHARMM36 predict realistic binding affinity. None of the tested models has the required accuracy to interpret the Ca^{2+}:lipid stoichiometry or induced structural changes with atomistic resolution.

In general, our results support the pre-2000 view that at submolar concentrations, in contrast to Ca^{2+} and other multivalent ions [1–4,10,11,19,20,27,29], Na^+ and other monovalent ions (except Li^+) do not specifically bind to phospholipid bilayers. Concerning the interpretation of existing experimental data, our work supports Cevc's view [2] that the observed small shift in phase transition temperature is not indicative of Na^+ binding. Further, our findings are in line with the noninvasive NMR spectroscopy work of Filippov et al. [11] that proved the results of Refs. 7,9,12 to be explainable by direct interactions between Na^+ ions and fluorescent probes. Finally, as spectroscopic methods are in general more sensitive to atomistic details in fluid-like environment than AFM, our work indirectly suggests that the ion binding reported from AFM experiments on fluid-like lipid bilayer systems [14–18] might be confounded with other physical features of the system. Concern-

ing contradictions in MD simulation results, we reinterpret strong Na^+ binding as an artefact of several simulation models, e.g., the Berger model used in Refs. 12,13.

The artificial specific Na^+ binding in simulations may lead to doubtful results, since it effectively leads to positively charged phosphatidylcholine (PC) lipid bilayers even at physiological NaCl concentration. Such a PC bilayer has distinctly different interactions with charged objects compared to a (more realistic) model without specific Na^+ binding. Furthermore, the overestimation of Na^+ binding affinity may extend also to other positively charged objects, say, membrane protein segments. This would affect lipid–protein interactions and could explain, for example, contradicting results on electrostatic interactions between charged protein segments and lipid bilayer [112,113]. In conclusion, more careful studies and model development on lipid bilayer–charged object interactions are called for to make molecular dynamics simulations directly usable in a physiologically relevant electrolytic environment.

This work has been done as a fully open collaboration, using `nmrlipids.blogspot.fi` as the communication platform. All the scientific contributions have been communicated publicly through this blog or GitHub repository [129]. All the related content and data is available at Ref. 129.

References

1 M. Eisenberg, T. Gresalfi, T. Riccio and S. McLaughlin, *Biochemistry*, 1979, **18**, 5213–5223.

2 G. Cevc, *Biochim. Biophys. Acta - Rev. Biomemb.*, 1990, **1031**, 311 – 382.

3 J.-F. Tocanne and J. Teissié, *Biochim. Biophys. Acta - Reviews on Biomembranes*, 1990, **1031**, 111 – 142.

4 H. Binder and O. Zschörnig, *Chem. Phys. Lipids*, 2002, **115**, 39 – 61.

5 J. J. Garcia-Celma, L. Hatahet, W. Kunz and K. Fendler, *Langmuir*, 2007, **23**, 10074–10080.

6 E. Leontidis and A. Aroti, *J. Phys. Chem. B*, 2009, **113**, 1460–1467.

7 R. Vacha, S. W. I. Siu, M. Petrov, R. A. Böckmann, J. Barucha-Kraszewska, P. Jurkiewicz, M. Hof, M. L. Berkowitz and P. Jungwirth, *J. Phys. Chem. A*, 2009, **113**, 7235–7243.

8 B. Klasczyk, V. Knecht, R. Lipowsky and R. Dimova, *Langmuir*, 2010, **26**, 18951–18958.

9 F. F. Harb and B. Tinland, *Langmuir*, 2013, **29**, 5540–5546.

10 G. Pabst, A. Hodzic, J. Strancar, S. Danner, M. Rappolt and P. Laggner, *Biophys. J.*, 2007, **93**, 2688 – 2696.

11 A. Filippov, G. Orädd and G. Lindblom, *Chem. Phys. Lipids*, 2009, **159**, 81 – 87.

12 R. A. Böckmann, A. Hac, T. Heimburg and H. Grubmüller, *Biophys. J.*, 2003, **85**, 1647 – 1655.

13 R. A. Böckmann and H. Grubmüller, *Ang. Chem. Int. Ed.*, 2004, **43**, 1021–1024.

14 S. Garcia-Manyes, G. Oncins and F. Sanz, *Biophys. J.*, 2005, **89**, 1812 – 1826.

15 S. Garcia-Manyes, G. Oncins and F. Sanz, *Electrochim. Acta*, 2006, **51**, 5029 – 5036.

16 T. Fukuma, M. J. Higgins and S. P. Jarvis, *Phys. Rev. Lett.*, 2007, **98**, 106101.

17 U. Ferber, G. Kaggwa and S. Jarvis, *Eur. Biophys. J.*, 2011, **40**, 329–338.

18 L. Redondo-Morata, G. Oncins and F. Sanz, *Biophys. J.*, 2012, **102**, 66 – 74.

19 R. J. Clarke and C. Lüpfert, *Biophys. J.*, 1999, **76**, 2614 – 2624.

20 H. Akutsu and J. Seelig, *Biochemistry*, 1981, **20**, 7366–7373.

21 J. N. Sachs, H. Nanda, H. I. Petrache and T. B. Woolf, *Biophys. J.*, 2004, **86**, 3772 – 3782.

22 M. L. Berkowitz, D. L. Bostick and S. Pandit, *Chem. Rev.*, 2006, **106**, 1527–1539.

23 A. Cordomí, O. Edholm and J. J. Perez, *J. Phys. Chem. B*, 2008, **112**, 1397–1408.

24 A. Cordomí, O. Edholm and J. J. Perez, *J. Chem. Theory Comput.*, 2009, **5**, 2125–2134.

25 C. Valley, J. Perlmutter, A. Braun and J. Sachs, *J. Membr. Biol.*, 2011, **244**, 35–42.

26 M. L. Berkowitz and R. Vacha, *Acc. Chem. Res.*, 2012, **45**, 74–82.

27 S. A. Tatulian, *Eur. J. Biochem.*, 1987, **170**, 413–420.

28 V. Knecht and B. Klasczyk, *Biophys. J.*, 2013, **104**, 818 – 824.

29 C. Altenbach and J. Seelig, *Biochemistry*, 1984, **23**, 3913–3920.

30 J. Seelig, P. M. MacDonald and P. G. Scherer, *Biochemistry*, 1987, **26**, 7535–7541.

31 P. G. Scherer and J. Seelig, *Biochemistry*, 1989, **28**, 7720–7728.

32 O. S. Ollila and G. Pabst, *Atomistic resolution structure and dynamics of lipid bilayers in simulations and experiments*, 2016, `http://dx.doi.org/10.1016/j.bbamem.2016.01.019`, In Press.

33 C. Altenbach and J. Seelig, *Biochim. Biophys. Acta*, 1985, **818**, 410 – 415.

34 P. M. Macdonald and J. Seelig, *Biochemistry*, 1987, **26**, 1231–1240.

35 M. Roux and M. Bloom, *Biochemistry*, 1990, **29**, 7077–7089.

36 G. Beschiaschvili and J. Seelig, *Biochim. Biophys. Acta - Biomembranes*, 1991, **1061**, 78 – 84.

37 F. M. Marassi and P. M. Macdonald, *Biochemistry*, 1992, **31**, 10031–10036.

38 J. R. Rydall and P. M. Macdonald, *Biochemistry*, 1992, **31**, 1092–1099.

39 T. M. Ferreira, R. Sood, R. Bärenwald, G. Carlström, D. Topgaard, K. Saalwächter, P. K. Kinnunen and S. O. Ollila, *Acyl chain disorder and azelaoyl orientation in lipid membranes containing oxidized lipids*, 0, http://dx.doi.org/10.1021/acs.langmuir.6b00788, PMID: 27260273.

40 M. Hong, K. Schmidt-Rohr and A. Pines, *J. Am. Chem. Soc.*, 1995, **117**, 3310–3311.

41 M. Hong, K. Schmidt-Rohr and D. Nanz, *Biophys. J.*, 1995, **69**, 1939 – 1950.

42 J. D. Gross, D. E. Warschawski and R. G. Griffin, *J. Am. Chem. Soc.*, 1997, **119**, 796–802.

43 A. Botan, F. Favela-Rosales, P. F. J. Fuchs, M. Javanainen, M. Kanduč, W. Kulig, A. Lamberg, C. Loison, A. Lyubartsev, M. S. Miettinen, L. Monticelli, J. Määttä, O. H. S. Ollila, M. Retegan, T. Róg, H. Santuz and J. Tynkkynen, *J. Phys. Chem. B*, 2015, **119**, 15075–15088.

44 J. Seelig, *Cell Biol. Int. Rep.*, 1990, **14**, 353–360.

45 A. A. Gurtovenko, M. Miettinen, , M. Karttunen and I. Vattulainen, *J. Phys. Chem. B*, 2005, **109**, 21126–21134.

46 W. Zhao, A. A. Gurtovenko, I. Vattulainen and M. Karttunen, *J. Phys. Chem. B*, 2012, **116**, 269–276.

47 M. S. Miettinen, A. A. Gurtovenko, I. Vattulainen and M. Karttunen, *J. Phys. Chem. B*, 2009, **113**, 9226–9234.

48 C. M. Franzin, P. M. Macdonald, A. Polozova and F. M. Winnik, *Biochim. Biophys. Acta - Biomembranes*, 1998, **1415**, 219 – 234.

49 S. Ollila, M. T. Hyvönen and I. Vattulainen, *J. Phys. Chem. B*, 2007, **111**, 3139–3150.

50 O. H. S. Ollila, T. Ferreira and D. Topgaard, *MD simulation trajectory and related files for POPC bilayer (Berger model delivered by Tieleman, Gromacs 4.5)*, 2014, {http://dx.doi.org/10.5281/zenodo.13279}.

51 T. P. Straatsma and H. J. C. Berendsen, *J. Chem. Phys*, 1988, **89**, year.

52 O. H. S. Ollila, *MD simulation trajectory and related files for POPC bilayer with 340mM NaCl (Berger model delivered by Tieleman, ffgmx ions, Gromacs 4.5)*, 2015, http://dx.doi.org/10.5281/zenodo.32144.

53 O. H. S. Ollila, *MD simulation trajectory and related files for POPC bilayer with 340mM CaCl_2 (Berger model delivered by Tieleman, ffgmx ions, Gromacs 4.5)*, 2015, http://dx.doi.org/10.5281/zenodo.32173.

54 S.-J. Marrink, O. Berger, P. Tieleman and F. Jähnig, *Biophys. J.*, 1998, **74**, 931 – 943.

55 J. Määttä, *DPPC_Berger*, 2015, http://dx.doi.org/10.5281/zenodo.13934.

56 J. Määttä, *DPPC_Berger_NaCl*, 2015, http://dx.doi.

57 J. Määttä, *DPPC_Berger_NaCl_1Mol*, 2015, http://dx.doi.org/10.5281/zenodo.17210.

58 D. P. Tieleman, J. L. MacCallum, W. L. Ash, C. Kandt, Z. Xu and L. Monticelli, *J. Phys. Condens. Matter*, 2006, **18**, S1221.

59 J. Määttä, *DPPC_Berger_OPLS06*, 2015, http://dx.doi.org/10.5281/zenodo.17237.

60 J. Åqvist, *J. Phys. Chem.*, 1990, **94**, 8021–8024.

61 J. Määttä, *DPPC_Berger_OPLS06_NaCl*, 2015, http://dx.doi.org/10.5281/zenodo.16484.

62 J. Määttä, *DPPC_Berger_OPLS06_NaCl_1Mol*, 2016, http://dx.doi.org/10.5281/zenodo.46152.

63 J. B. Klauda, R. M. Venable, J. A. Freites, J. W. O'Connor, D. J. Tobias, C. Mondragon-Ramirez, I. Vorobyov, A. D. M. Jr and R. W. Pastor, *J. Phys. Chem. B*, 2010, **114**, 7830–7843.

64 O. H. S. Ollila and M. Miettinen, *MD simulation trajectory and related files for POPC bilayer (CHARMM36, Gromacs 4.5)*, 2015, {http://dx.doi.org/10.5281/zenodo.13944}.

65 R. M. Venable, Y. Luo, K. Gawrisch, B. Roux and R. W. Pastor, *J. Phys. Chem. B*, 2013, **117**, 10183–10192.

66 O. H. S. Ollila, *MD simulation trajectory and related files for POPC bilayer with 350mM NaCl (CHARMM36, Gromacs 4.5)*, 2015, http://dx.doi.org/10.5281/zenodo.32496.

67 O. H. S. Ollila, *MD simulation trajectory and related files for POPC bilayer with 690mM NaCl (CHARMM36, Gromacs 4.5)*, 2015, http://dx.doi.org/10.5281/zenodo.32497.

68 O. H. S. Ollila, *MD simulation trajectory and related files for POPC bilayer with 950mM NaCl (CHARMM36, Gromacs 4.5)*, 2015, http://dx.doi.org/10.5281/zenodo.32498.

69 M. Girych and O. H. S. Ollila, *POPC_CHARMM36_CaCl2_035Mol*, 2015, http://dx.doi.org/10.5281/zenodo.35159.

70 M. Javanainen, *POPC @ 310K, 450 mM of CaCl_2. Charmm36 with default Charmm ions*, 2016, http://dx.doi.org/10.5281/zenodo.51185.

71 M. Girych and O. H. S. Ollila, *POPC_CHARMM36_CaCl2_067Mol*, 2015, http://dx.doi.org/10.5281/zenodo.35160.

72 M. Girych and O. H. S. Ollila, *POPC_CHARMM36_CaCl2_1Mol*, 2015, http://dx.doi.org/10.5281/zenodo.35156.

73 J. Yoo, J. Wilson and A. Aksimentiev, *Biopolymers*, 2016.

74 A. Maciejewski, M. Pasenkiewicz-Gierula, O. Cramariuc, I. Vattulainen and T. Rog, *J. Phys. Chem. B*, 2014, **118**, 4571–4581.

75 M. Javanainen, 2014.

76 M. Javanainen, *POPC @ 310K, varying amounts of NaCl. Model by Maciejewski and Rog*, 2015, http://dx.doi.org/10.5281/zenodo.14976.

77 O. H. S. Ollila, J. Määttä and L. Monticelli, *MD simulation trajectory for POPC bilayer (Orange, Gromacs 4.5.)*, 2015, http://dx.doi.org/10.5281/zenodo.34488.

78 O. H. S. Ollila, J. Määttä and L. Monticelli, *MD simula-*

tion trajectory for POPC bilayer with 140mM NaCl (Orange, Gromacs 4.5.)*, 2015, http://dx.doi.org/10.5281/zenodo.34491.

79 O. H. S. Ollila, J. Määttä and L. Monticelli, *MD simulation trajectory for POPC bilayer with 510mM NaCl (Orange, Gromacs 4.5.)*, 2015, http://dx.doi.org/10.5281/zenodo.34490.

80 S. Ollila, J. Määttä and L. Monticelli, *MD simulation trajectory for POPC bilayer with 1000mM NaCl (Orange, Gromacs 4.5.)*, 2015, http://dx.doi.org/10.5281/zenodo.34497.

81 O. H. S. Ollila, J. Määttä and L. Monticelli, *MD simulation trajectory for POPC bilayer with 510mM CaCl_2 (Orange, Gromacs 4.5.)*, 2015, http://dx.doi.org/10.5281/zenodo.34498.

82 J. P. M. Jämbeck and A. P. Lyubartsev, *J. Phys. Chem. B*, 2012, **116**, 3164–3179.

83 J. Määttä, *DPPC_Slipids*, 2014, http://dx.doi.org/10.5281/zenodo.13287.

84 D. Beglov and B. Roux, *J. Chem. Phys.*, 1994, **100**, 9050–9063.

85 B. Roux, *Biophys. J.*, 1996, **71**, 3177 – 3185.

86 J. Melcr, *Simulation files for DPPC lipid membrane with Slipids force field for Gromacs MD simulation engine*, 2016, http://dx.doi.org/10.5281/zenodo.55322.

87 J. P. M. Jämbeck and A. P. Lyubartsev, *J. Chem. Theory Comput.*, 2012, **8**, 2938–2948.

88 M. Javanainen, *POPC @ 310K, Slipids force field.*, 2015, DOI: 10.5281/zenodo.13887.

89 D. E. Smith and L. X. Dang, *J. Chem. Phys*, 1994, **100**, year.

90 M. Javanainen, *POPC @ 310K, 130 mM of NaCl. Slipids with ions by Smith & Dang*, 2015, http://dx.doi.org/10.5281/zenodo.35275.

91 M. Javanainen, *POPC @ 310K, 450 mM of CaCl_2. Slipids with default Amber ions*, 2016, http://dx.doi.org/10.5281/zenodo.51182.

92 C. J. Dickson, B. D. Madej, Ã. A. Skjevik, R. M. Betz, K. Teigen, I. R. Gould and R. C. Walker, *J. Chem. Theory Comput.*, 2014, **10**, 865–879.

93 M. Girych and O. H. S. Ollila, *POPC_AMBER_LIPID14_Verlet*, 2015, http://dx.doi.org/10.5281/zenodo.30898.

94 M. Girych and O. H. S. Ollila, *POPC_AMBER_LIPID14_NaCl_015Mol*, 2015, http://dx.doi.org/10.5281/zenodo.30891.

95 M. Girych and O. H. S. Ollila, *POPC_AMBER_LIPID14_NaCl_1Mol*, 2015, http://dx.doi.org/10.5281/zenodo.30865.

96 M. Girych and O. H. S. Ollila, *POPC_AMBER_LIPID14_CaCl2_035Mol*, 2015, http://dx.doi.org/10.5281/zenodo.34415.

97 M. Girych and O. H. S. Ollila, *POPC_AMBER_LIPID14_CaCl2_1Mol*, 2015, http://dx.doi.org/10.5281/zenodo.35074.

98 J. P. Ulmschneider and M. B. Ulmschneider, *J. Chem. Theory Comput.*, 2009, **5**, 1803–1813.

99 M. Girych and O. H. S. Ollila, *POPC_Ulmschneider_OPLS_Verlet_Group*, 2015, http://dx.doi.org/10.5281/zenodo.30904.

100 M. Girych and O. H. S. Ollila, *POPC_Ulmschneider_OPLS_NaCl_015Mol*, 2015, http://dx.doi.org/10.5281/zenodo.30892.

101 M. Girych and O. H. S. Ollila, *POPC_Ulmschneider_OPLS_NaCl_1Mol*, 2015, http://dx.doi.org/10.5281/zenodo.30894.

102 H. Hauser, M. C. Phillips, B. Levine and R. Williams, *Nature*, 1976, **261**, 390 – 394.

103 H. Hauser, W. Guyer, B. Levine, P. Skrabal and R. Williams, *Biochim. Biophys. Acta - Biomembranes*, 1978, **508**, 450 – 463.

104 L. Herbette, C. Napolitano and R. McDaniel, *Biophys. J.*, 1984, **46**, 677 – 685.

105 B. Hess, C. Holm and N. van der Vegt, *J. Chem. Phys*, 2006, **124**, year.

106 A. A. Chen, and R. V. Pappu, *J. Phys. Chem. B*, 2007, **111**, 11884–11887.

107 M. M. Reif, M. Winger and C. Oostenbrink, *J. Chem. Theory Comput.*, 2013, **9**, 1247–1264.

108 I. Leontyev and A. Stuchebrukhov, *Phys. Chem. Chem. Phys.*, 2011, **13**, 2613–2626.

109 W. L. Jorgensen, D. S. Maxwell and J. Tirado-Rives, *J. Am. Chem. Soc.*, 1996, **118**, 11225–11236.

110 M. Kohagen, P. E. Mason and P. Jungwirth, *J. Phys. Chem. B*, 2016, **120**, 1454–1460.

111 M. Kohagen, P. E. Mason and P. Jungwirth, *J. Phys. Chem. B*, 2014, **118**, 7902–7909.

112 A. Arkhipov, Y. Shan, R. Das, N. Endres, M. Eastwood, D. Wemmer, J. Kuriyan and D. Shaw, *Cell*, 2013, **152**, 557 – 569.

113 K. Kaszuba, M. Grzybek, A. Orlowski, R. Danne, T. Róg, K. Simons, Ã. Coskun and I. Vattulainen, *Proc. Natl. Acad. Sci. USA*, 2015, **112**, 4334–4339.

114 M. S. Miettinen, *Molecular dynamics simulation trajectory of a fully hydrated DMPC lipid bilayer*, 2013, http://dx.doi.org/10.5281/zenodo.51635.

115 M. S. Miettinen, *Molecular dynamics simulation trajectory of a cationic lipid bilayer: 6/94 mol% DMTAP/DMPC*, 2016, http://dx.doi.org/10.5281/zenodo.51639.

116 M. S. Miettinen, *Molecular dynamics simulation trajectory of a cationic lipid bilayer: 50/50 mol% DMTAP/DMPC*, 2016, http://dx.doi.org/10.5281/zenodo.51748.

117 J. Määttä, *DPPC_Berger_NaCl_scaled*, 2015, {http://dx.doi.org/10.5281/zenodo.16320}.

118 J. Määttä, *DPPC_Berger_NaCl_1Mol_scaled*, 2015, http://dx.doi.org/10.5281/zenodo.17228.

119 J. Määttä, *DPPC_Berger_OPLS06_NaCl_scaled*, 2015, {http://dx.doi.org/10.5281/zenodo.16485}.

120 J. Määttä, *DPPC_Berger_OPLS06_NaCl_1Mol_scaled*, 2015, http://dx.doi.org/10.5281/zenodo.17209.

121 M. Javanainen, *POPC @ 310K, varying amounts of NaCl. Slipids with ECC-scaled ions*, 2015, `http://dx.doi.org/10.5281/zenodo.35193`.

122 M. Javanainen, *POPC @ 310K, 450 mM of CaCl_2. Charmm36 with ECC-scaled ions*, 2016, `http://dx.doi.org/10.5281/zenodo.45008`.

123 M. Javanainen, *POPC @ 310K, 450 mM of CaCl_2. Slipids with ECC-scaled ions*, 2016, `http://dx.doi.org/10.5281/zenodo.45007`.

124 J. Melcr, *Simulation files for POPC lipid membrane with Charmm36 force field without NBFIX for Gromacs MD simulation engine*, 2016, `http://dx.doi.org/10.5281/zenodo.55318`.

125 S. Pronk, S. Páll, R. Schulz, P. Larsson, P. Bjelkmar, R. Apostolov, M. R. Shirts, J. C. Smith, P. M. Kasson, D. van der Spoel, B. Hess and E. Lindahl, *Bioinformatics*, 2013, **29**, 845–854.

126 M. J. Abraham, T. Murtola, R. Schulz, S. Páll, J. C. Smith, B. Hess and E. Lindahl, *SoftwareX*, 2015, **1-2**, 19–25.

127 J. C. Phillips, R. Braun, W. Wang, J. Gumbart, E. Tajkhorshid, E. Villa, C. Chipot, R. D. Skeel, L. Kalé and K. Schulten, *J. Comput. Chem.*, 2005, **26**, 1781–1802.

128 D. van der Spoel, E. Lindahl, B. Hess, A. R. van Buuren, E. Apol, P. J. Meulenhoff, D. P. Tieleman, A. L. T. M. Sijbers, K. A. Feenstra, R. van Drunen and H. J. C. Berendsen, *GROMACS user manual version 4.0*, 2005.

129 O. H. S. Ollila and et al., 2015, `https://github.com/NMRLipids/lipid_ionINTERACTION`.

130 T. M. Ferreira, F. Coreta-Gomes, O. H. S. Ollila, M. J. Moreno, W. L. C. Vaz and D. Topgaard, *Phys. Chem. Chem. Phys.*, 2013, **15**, 1976–1989.

131 O. Berger, O. Edholm and F. Jähnig, *Biophys. J.*, 1997, **72**, 2002 – 2013.

132 M. Bachar, P. Brunelle, D. P. Tieleman and A. Rauk, *J. Phys. Chem. B*, 2004, **108**, 7170–7179.

133 B. Hess, H. Bekker, H. J. C. Berendsen and J. G. E. M. Fraaije, *J. Comput. Chem.*, 1997, **18**, 1463–1472.

134 B. Hess, *J. Chem. Theory Comput.*, 2008, **4**, 116–122.

135 T. Darden, D. York and L. Pedersen, *J. Chem. Phys*, 1993, **98**, year.

136 U. L. Essman, M. L. Perera, M. L. Berkowitz, T. Larden, H. Lee and L. G. Pedersen, *J. Chem. Phys.*, 1995, **103**, 8577–8592.

137 G. Bussi, D. Donadio and M. Parrinello, *J. Chem. Phys*, 2007, **126**, year.

138 M. Parrinello and A. Rahman, *J. Appl. Phys.*, 1981, **52**, 7182–7190.

139 H. J. C. Berendsen, J. P. M. Postma, W. F. van Gunsteren, A. DiNola and J. R. Haak, *J. Chem. Phys.*, 1984, **81**, 3684–3690.

140 S. Nose, *Mol. Phys.*, 1984, **52**, 255–268.

141 W. G. Hoover, *Phys. Rev. A*, 1985, **31**, 1695–1697.

142 J. Lee, X. Cheng, J. M. Swails, M. S. Yeom, P. K. Eastman, J. A. Lemkul, S. Wei, J. Buckner, J. C. Jeong, Y. Qi, S. Jo, V. S. Pande, D. A. Case, I. Charles L. Brooks, J. Alexander D. MacKerell, J. B. Klauda and W. Im, *J. Chem. Theory Comput.*, 2016, **12**, 405–413.

143 S. Páll and B. Hess, *Computer Physics Communications*, 2013, **184**, 2641 – 2650.

144 W. L. Jorgensen, J. Chandrasekhar, J. D. Madura, R. W. Impey and M. L. Klein, *J. Chem. Phys*, 1983, **79**, year.

145 L. Martínez, R. Andrade, E. G. Birgin and J. M. Martínez, *J. Comput. Chem.*, 2009, **30**, 2157–2164.

146 W. Humphrey, A. Dalke and K. Schulten, *J. Mol. Graphics*, 1996, **14**, 33–38.

147 M. Abraham, D. van der Spoel, E. Lindahl, B. Hess and the GROMACS development team, *GROMACS user manual version 5.0.7*, 2015.

148 W. L. Jorgensen, J. D. Madura and C. J. Swenson, *J. Am. Chem. Soc.*, 1984, **106**, 6638–6646.

149 W. L. Jorgensen and J. Gao, *J. Phys. Chem.*, 1986, **90**, 2174–2182.

150 W. L. Jorgensen, *J. Phys. Chem.*, 1986, **90**, 1276–1284.

151 W. L. Jorgensen and J. Tirado-Rives, *J. Am. Chem. Soc.*, 1988, **110**, 1657–1666.

152 J. M. Briggs, T. B. Nguyen and W. L. Jorgensen, *J. Phys. Chem.*, 1991, **95**, 3315–3322.

153 O. H. S. Ollila and M. Retegan, *MD simulation trajectory and related files for POPC bilayer (Lipid14, Gromacs 4.5)*, 2014, `http://dx.doi.org/10.5281/zenodo.12767`.

154 J. Domański, P. Stansfeld, M. Sansom and O. Beckstein, *J. Membr. Biol.*, 2010, **236**, 255–258.